IMPACT OF TRANSPORTATION ON SILICON WAFER-BASED PV MODULES

Marc Köntges[1], Michael Siebert[1], Alejandro de la Dedicación Rodríguez[1], Martin Denz[2], Martin Wegner[3], Romy Illing[4], Frank Wegert[4]
[1] Institute for Solar Energy Research Hamelin (ISFH), Am Ohrberg 1, D-31860 Emmerthal, Germany
Tel: +49 5151 999 432; Fax: +49 5151 999 400; Email: Koentges@isfh.de
[2]alfasolar GmbH, Ahrensburger Straße 4-6, D-30659 Hannover, Germany
[3]Conergy SolarModule GmbH & Co. KG, Conergy-Straße 8, D-15236 Frankfurt (Oder), Germany
[4]Q-Cells SE, Sonnenallee 17-21, 06766 Bitterfeld-Wolfen, Germany, now with Hanwha Q.Cells GmbH, Sonnenallee 17-21, 06766 Bitterfeld-Wolfen, Germany

ABSTRACT: Before a PV module is integrated into a PV system it has to be handled and transported. This part of a PV module's life causes some direct returns mostly due to glass breakage. But even when the glass is not broken the mechanical loads may cause cell cracks in some cases. The cell cracks typically have a very low direct impact on the PV module performance, but may reduce the durability of the PV module power. Therefore it is imperative to test the PV module for typical load situations occurring during the transport. There is already a standard to test transport units of PV modules. However for the development of PV modules this test is quite unsuitable, because the developer does not know the loads occurring at the module and one must test a whole stack of modules which are often not accessible at the development stage. Therefore we measured the accelerations of PV module corners during transport handling and transport for well packed horizontal PV module stacks. For German country roads we found the highest random vibrations during a transport with a truck company. The reduced power spectral density (PSD) of this random vibration is quite similar to the PSD spectrum suggested for testing of PV module packages in IEC62759-1. We use this PSD to test the PV modules on a shaker being attached at the corners of the module to simulate the situation in the stack. However the suggested test in that standard produces much more cell cracks than found in the transports where the PSD was generated from. Besides the PSD spectrum we also measured shocks during the transport. An analysis of different sine shocks shows that only shocks of a specific shock length of about 40 ms and about 20 ms and maximum amplitude higher than 20 m/s can affect the PV modules. We suggest a combined application of the shocks and PSD test procedure to reproduce realistic transport conditions.

Keywords: PV module, transport, shipping, cell crack, shaker

1 INTRODUCTION

In previous publications, transportation has been discussed to be a source of solar cell cracking in photovoltaic (PV) modules [1, 2]. This cell cracking may reduce the reliability of the solar modules [3, 4]. In this paper we try to quantify and assess the cell cracking caused by movement of the PV modules during transportation and transport handling. First we identify which of the movement stages are most challenging for the cracking of solar cells in a PV module. Subsequently we create a test to simulate the transport stress for single solar modules and analyze the cell cracking behavior.
With these tests we want to answer the following questions:
1. How do the frequency distribution of shocks and the power density spectrum (PSD) look like of road transports in Germany?
2. Is there an acceleration threshold beyond no PV module shows cell cracks?
3. How much do the cell cracks affect the PV module power?
4. Are the PV modules prone to special shock forms?
5. How can we assess arbitrary shock forms and the PSD spectrum in realistic transports?
6. How should we test single PV modules for transport?

2 EXPERIMENTAL SETUP

In this work we focus on 60 cell modules with a cell size of 15.6 cm x 15.6 cm, a glass cover and a back sheet foil. In this study all tested modules are stacked horizontally with sunny side down. All used transport packages are designed for the particular module type. No inadequate package is used. Inadequate package easily leads to more damage than reported here.

Field setup

To assess the influence of transportation to the cracking behavior and the module power of PV modules we attend several PV module transports. In this work we focus on PV-modules transported in the manufacturer packaging and proper securing of the module stack in the truck. The packages used in this study assure that the bottom module is fully supported by the shipment corners and in any case not touched by the module pallet. We use one general setup for the measurement of the vibrations and shocks. Fig. 1 shows the positioning of the sensors during the transportation. For the logging of the acceleration of the modules we use two kinds of sensors. We use the calibrated acceleration logger ShockLog 298 from LAMERHOLM to measure shocks at the pallet. The ShockLog 298 is quite heavy with 550 g. This data logger filters its input signal by a 250 Hz low pass filter. To avoid an influence of the logger to the vibration of the PV modules we use an uncalibrated data logger MSR 165 to log the vibration on the PV modules. This logger weights only 69 g. We calibrate the MSR 165 on our shaker at 10 Hz with an effective 1 *g* and 10 *g* sine wave against the calibrated shaker sensors. For shock measurements the MSR 165 is used in a shock mode. In the shock mode both sensors are programmed to start logging after an acceleration of at least 3 *g*. For vibration measurements we connect the MSR 165 to a self made remote control

that we can measure vibrations for 10 s. For that purpose we follow the truck with a car to document the route section and start the sensor by a remote control. The MSR 165 does not filter the input signal. Therefore the reading of the MSR 165 is filtered after logging by a digital 250 Hz low and a 1 Hz high pass filter.

From the shock acceleration data the root mean square acceleration a_{RMS} is calculated from the acceleration peak with the highest amplitude in a dataset by

$$a_{RMS} = \max_{1\le i\le n}\left(\sqrt[2]{\frac{\sum_{j=t_{a=0}(i)}^{t_{a=0}(i+1)} a^2(j)}{t_{a=0}(i+1)-t_{a=0}(i)+1}}\right). \qquad (1)$$

The function a(j) describes the measured acceleration at each measuring point j. The enumerator i counts the number of zero crossings of the acceleration signal in the measured time interval until the last zero crossing n. The measuring points $t_{a=0}$(i) are the corresponding measurement points where the acceleration signal crosses zero. Due to this method it is assured that only the peak with the highest a_{RMS} value is used for the evaluation. Therefore pre- and after-shocks are not considered. In transportation analysis the accelerations are typically scaled by the gravity acceleration. Therefore we define g_{RMS} by

$$g_{\mathrm{RMS}} := \frac{a_{\mathrm{RMS}}}{9.81\frac{\mathrm{m}}{\mathrm{s}}}\ . \qquad (2)$$

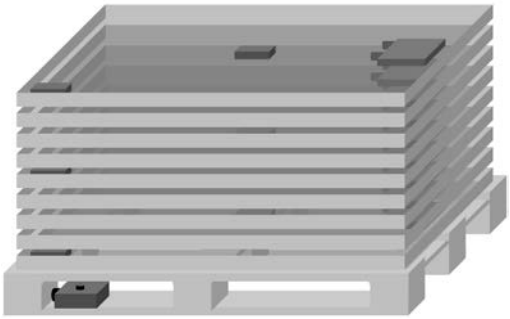

Fig. 1: The sketch shows the standard positions of the data logger for the acquisition of acceleration data in a PV module transport stack. The logger ShockLog 298 is screwed in the corner of the pallet. Each module in the bottom, in the middle and in the top position is equipped with two MSR 165 data logger. They are taped with double sided carpet tape on the module back sheet. On the above-mentioned PV modules one logger is positioned in the module middle and one logger in the module corner. The logger in the module corner is located in the opposite corner of the junction box directly above the ShockLog 298. The ShockLog also acquires the ambient temperature. During all real life transports we measured temperatures in the range of 1°C to 34°C.

Shaker Setup

To assess the influence of vibrations on PV modules we setup a shaker system to simulate vibrations of PV modules. We use the shaker system SW 8142 from "Regelungs- und Messtechnik Dipl.-Ing. Schäfer GmbH & Co. KG" (RMS) to excite the vibration of PV modules. To measure the acceleration of the modules we use the calibrated acceleration sensors 8640A10 and 8640A50 from Kistler. These sensors are very lightweight so they do not influence the vibration of the PV module.

The shaker inclusive expander platform is free of resonance frequencies in the range of 3 Hz to 140 Hz. To test the cracking sensitivity of seven types of PV modules to transportation we tested single PV modules mounted on the shaker platform. The module is mounted on the shaker sunny side down by rigid fixing the PV module corners as it is done in a module transport stack. The reference sensor for the shaker control is located close to one PV module corner at the module mounting. Fig. 2 shows a photograph of the used shaker setup including a mounted test specimen.

Fig. 2: Photograph of the shaker setup.

To measure the maximum deflection of the middle of the PV module relative to the shaker expander platform a laser distance analyzer OWLE 5013 AA S1 from Weleotec, is mounted rigid on the expander platform. The maximum module deflection is the distance between the maximum and minimum deflection of the module middle measured in a shock test. To record the readings with a computer we use a REDLAB 1208LS from Meilhaus Electronic. The total error of a distance reading is ±0.3 mm with a confidence level of 95%.

We use two different test sequences in this work:

1. PSD test to test the effect of random vibrations to the cells of one single PV module
2. Shock test to test the effect of single shock events to the cells of one single PV module

To create a test PSD-spectrum for single PV modules we measure the vibration of the PV modules and create according to standard DIN EN 15433-5 Feb2008 a reduced PSD.

For the shock test we choose a sinusoidal time dependence of the acceleration at the corners of the PV module. The shock form is defined as:

$$a(t) = a_{\max}\cdot\sin(t) \text{ for } 0 < t < t_{\max}. \qquad (3)$$

We vary the maximum amplitude $a_{\max}$ of the shock in five steps 5 m/s², 10 m/s², 20 m/s² and 30 m/s². For sinusoidal shock forms

$$a_{\mathrm{RMS}} = \frac{1}{\sqrt{2}}\, a_{\max} \qquad (4)$$

describes the relation between the maximum acceleration and the root mean square acceleration.

For each amplitude we vary the shock length t_{max} from 2 ms up to 36.5 ms in steps of 1.5 ms. Furthermore testes are done with shock length of 40 ms and 45 ms. In the following the inverse of the double of the shock width is named corresponding shock frequency *f*

$$f = \frac{1}{2t_{max}}. \quad (5)$$

We conduct the test in accordance to standard DIN-EN-60068-2-27, but we allow the shaker a preshock level of 30% of the main shock to avoid resonances of the shaker at high shock length of 40 ms and 45 ms. For each shock parameter set we conduct 5 shocks per PV module. Before the main shock test shocks are applied to the module to teach the controller. Test shocks are started at -18 dB of the main shock level and are increased in steps of 1.5 dB or 0.75 dB up to the target shock level. Between all shocks the PV module has 4 s to settle.

Counting and classifying cell cracks

For the counting of cell cracks we use the differential electroluminescence (EL) method which reveals even small cell cracks in multi crystalline solar cells. We record the EL image of the PV modules in the initial state and after any test procedure at the nominal current of the module. Subsequently we subtract both EL images. A high quality alignment of the two images is achieved by applying image registration techniques before comparison of both images. The method is already used in former crack analysis [5]. To characterize the direct impact of the crack on the PV module power we classify the cracked cells according to the cell crack classes A (no electrical loss over the crack), B (crack with electrical losses) and C (electrical isolating crack) defined in previous work [3].

Measuring the power loss due to shaker tests

Before and after a test sequence the output power of the PV module is measured by a cetis class AAA HALM flasher with a reproducibility of ±0.1% in module power for repeated measurements at standard test conditions.

3 RESULTS AND DISCUSSION

3.1 Shock results from the field

In Fig. 3 we compare the shock intensity and occurrence for a) transport handling, b) a full loaded 40-ton truck and c) transport done by a truck company with an unknown truck type. The 40-ton truck and the truck company transported the PV modules over the same distance in Germany. The transport handling and the truck company transport of Fig. 3 a) and c) are taken from the same transport. The results show that during the transport handling shocks with the highest intensity occur to the pallet, but not to the PV modules. The handling includes the module stacking onto the pallet, the movement, lift and settling with the pallet truck and the dismantling of the pallet stack. The full loaded 40-ton truck transport shows shocks with low intensity and low occurrence. The transportation with the truck company shows the highest shock intensity for the modules and the highest shock frequency. So we focus on that worst case transport (truck company) in this work. The frequency distribution of the truck company is scaled by the factor 0.9^{-1} because 10% of the measured data is lost. The MSR 165 sensors generate high shock frequencies at low g_{RMS} levels because the trigger is activated before the shock acceleration signal is filtered. After the transport handling and shipment depicted in Fig. 3 a) and c) we found the cell crack distribution shown in Fig. 4. The highest number of cell cracks per module is two. There is still the uncertainty that we cannot differentiate in the test between cell cracks caused by the transport handling and the transport itself.

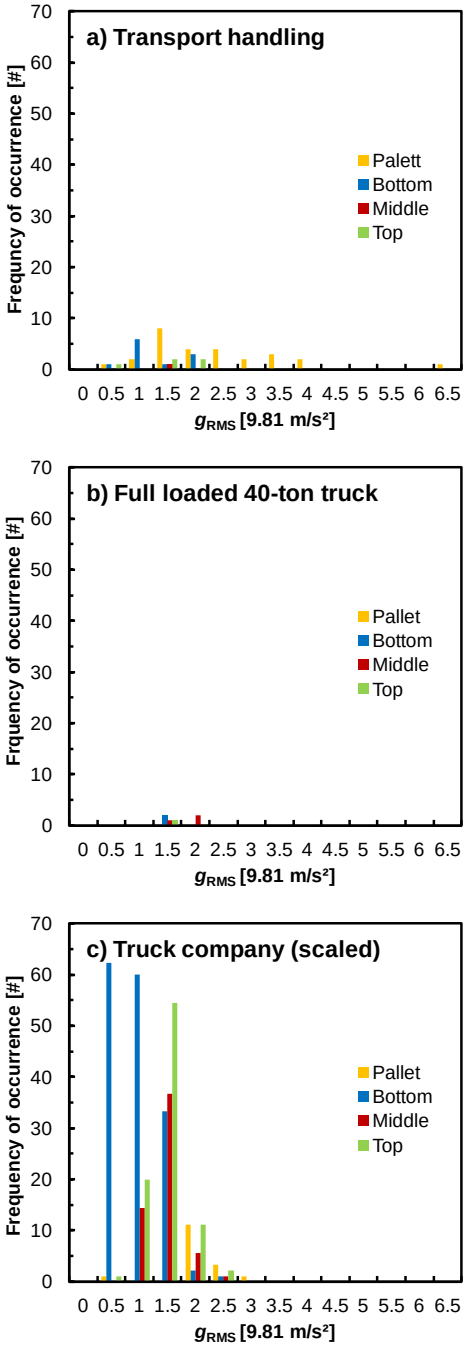

Fig. 3: Measured shock occurrence for a) transport handling, b) transport in full loaded 40-ton truck and c) transport with a truck company driving the same distance. Pallet, bottom, middle and upper indicate the measurement at the module positions at the pallet and in the bottom, middle and upper part of packaging unit.

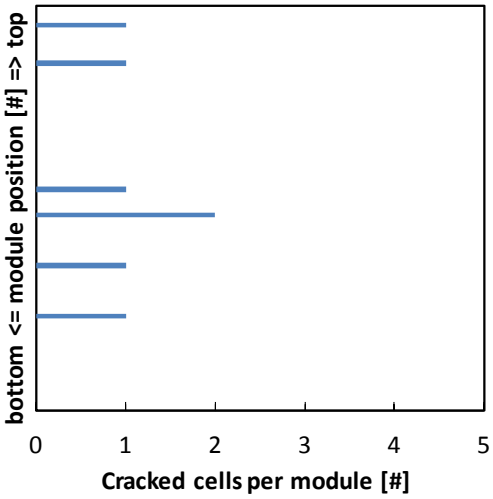

Fig. 4: Some PV modules in the transport stack show one or two cell cracks per PV module after the transport. This statistic belongs to the same transport being evaluated in Fig. 3 a) and c).

3.2 Shock results from the lab

Fig. 5 shows the maximum deflection of the middle position of a PV module as function of the correspondent frequency of the sinusoidal shock for one PV module sample. From now on this function is called deflection function $A_S(f)$. The amplitude of the module middle scales linearly with the shock amplitude as shown in Fig. 6. Therefore we simplify the description of the shock response of the module middle by one normalized deflection function $A_S(f)/a_{max}$. The normalized deflection function describes the maximal amplitude of the PV module middle in dependence of the corresponding frequency of the sinusoidal shock.

Fig. 7 shows the normalized deflection as function of the corresponding shock frequency for five module types used in this work. The corresponding frequency of the maximum amplitudes of the PV modules shifts slightly from PV module type to PV module type. However the range of relevant frequencies is almost the same for all tested modules. The most relevant corresponding frequency ranges for high module deflections are 11 Hz - 15 Hz (~40 ms) and 20 Hz - 35 Hz (~20 ms). The maximum deflection amplitude per acceleration varies about ±10% for the 7 module types.

Fig. 8 shows the cell cracking occurrence as function of the maximum deflection of all PV module types used in this work. Only deflections of 20 mm and more result in some cases in cell cracks. For the module type used for the evaluation in Fig. 3 a) and c) we found the first crack occurrence at a deflection of 24.4 mm. Some modules do not show in any case cell cracks, even for deflections up to 25 mm. This finding and Fig. 5 visualize that the cell cracking behavior is not only depending of the maximum acceleration of the shock. The most relevant parameter is the maximum module deflection which is linked to the shock form by the normalized deflection function given in Fig. 7.

All tested modules do not show any measurable power loss after the shock test.

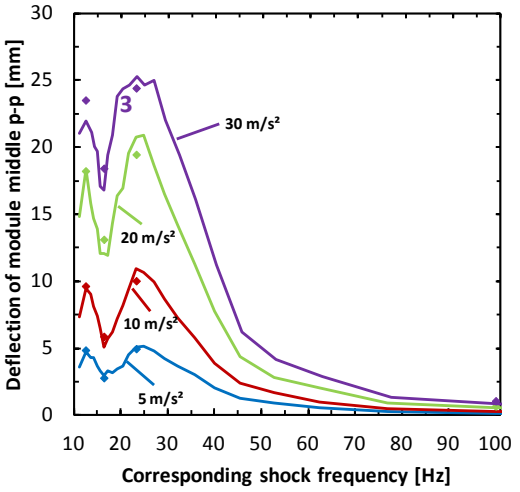

Fig. 5: Maximum deflection of the middle position of the PV module type used in section 3.1 as function of the correspondent shock frequency of the sinusoidal shock. The maximum sinus shock acceleration is given as parameter in the figure. The single points represent reproduction test where the cell cracks are counted after the test (please also recognize the points at 100 Hz). A number below the points shows the number of cell cracks that occurred at that specific shock. No number means no cell crack occurs.

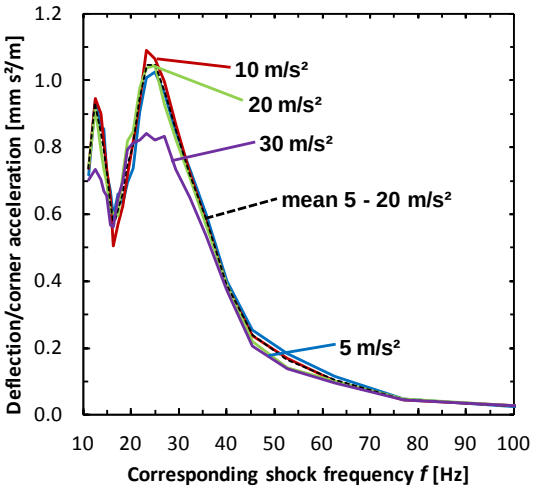

Fig. 6: The functions given in Fig. 5 scaled by the corresponding shock amplitude a_{max} given as parameter in the graph. Up to a_{max} = 20 m/s² peak acceleration all functions scale linear with the shock amplitude. For 30 m/s² the functions still scale linear except for the peak regions.

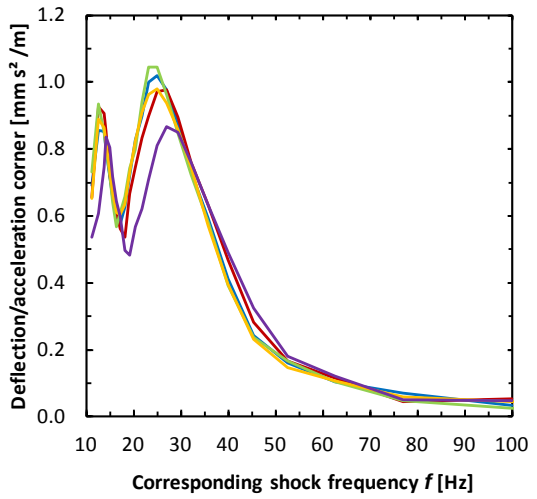

Fig. 7: Normalized deflection functions as function of the corresponding shock frequency for 5 different module types.

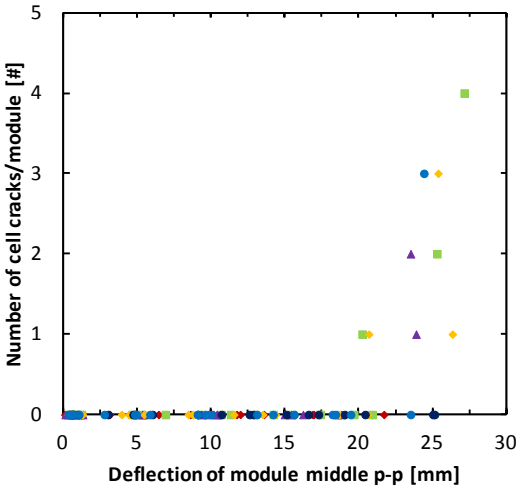

Fig. 8: Correlation of the maximum deflection of the module to the number of generated cell cracks. Different points represent different PV module types, shocked for several amplitudes a_{max} and corresponding shock frequencies f resulting in a certain deflection.

3.3 Discussion of shock results from the lab

By assuming that various sinus shocks being applied to a PV module do not interact with each other we can use the deflection function as transfer function for arbitrary shock forms:

$$A_M(f) = a_M(f) \cdot \left(\frac{A_S(f)}{a_{max}}\right). \quad (6)$$

The symbol $A_S(f)$ represent the measured deflection function as shown in Fig. 5, a_{max} is the is the maximum acceleration amplitude for that the deflection spectrum $A_S(f)$ has been measured, $a_M(f)$ is the acceleration spectrum during a transport shock measured at a module corner and $A_M(f)$ is the resulting amplitude in the module middle during the transport. With the normalized transfer function of the PV module shown in Fig. 6 the shocks counted in Fig. 3 a) and c) are transferred by Eq. (6) into deflection amplitudes of the PV module middle. Fig. 9 shows the resulting deflection histogram for the realistic transport handling and truck company transport. In this case the transport handling does not show any relevant shock for the modules but the module transport shows two events above the cell crack level of the module type. During this transport at maximum two cell cracks occurred per module, some with one cell crack, but most modules have no cell crack. This result is comparable with the lab result.

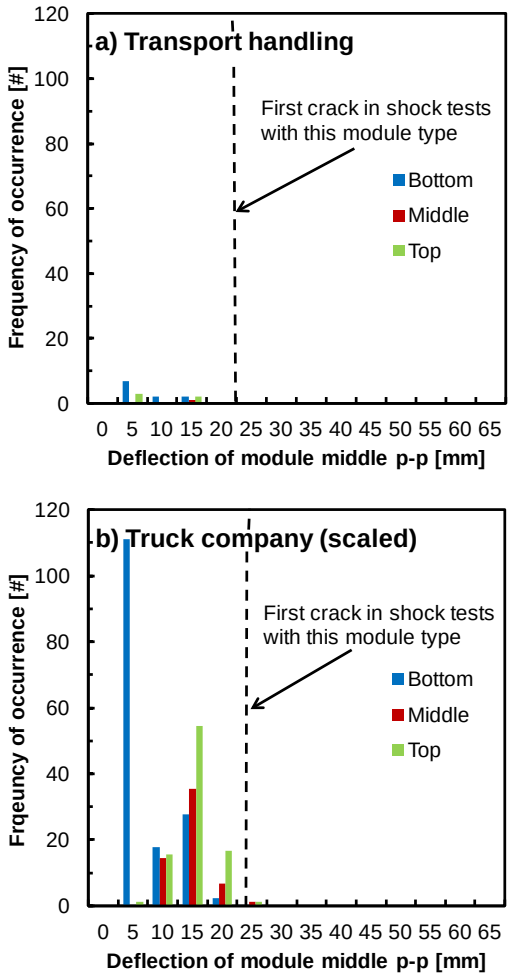

Fig. 9: Deflection occurrence for a truck company transport calculated by applying the mean transfer function of Fig. 5 with Eq. (2) to the base acceleration data used to generate Fig. 3 c). For that module type the dashed line indicates the module deflection where the first cell cracking occurs in the shock tests, compare Fig. 8.

3.3 Vibration results from the field

Fig. 10 shows the reduced PSDs for the upper and bottom module in the transport stack. This analysis is done for city, country road and autobahn. The country road exhibit the highest reduced PSD for the upper module. Especially for the country road the trucks are sent by us along the worst roads we know. The resulting reduced PSD spectra are quite high. As the highest measured PSD has the highest impact on the reduced PSD spectrum already one rough road increases the reduced PSD spectrum a lot. However a comparison with

existing standards shows a good agreement with the PSD spectrum form of the ASTM D4169-09 Truck Assurance Level II with 0.52 g_{RMS}. This spectrum is also used in the current transport standard for PV module packages [6]. The standard spectrum is used in the following to test single PV modules on a shaker. The highest PSD level is found for the top modules. This result coincidence with the highest shock level and highest shock occurrence at the top module shown in Fig. 3.

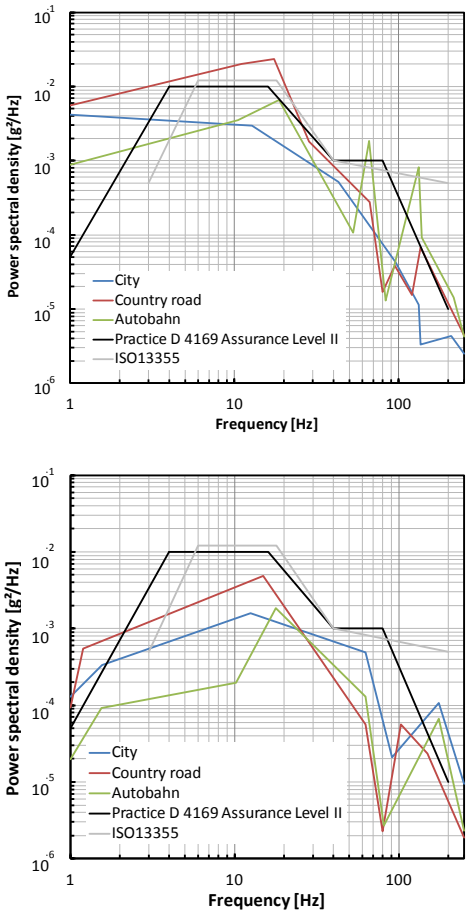

Fig. 10: Measured reduced PSDs of a transport stack for sunny side down stacked PV modules. The PSD is measured in the corners of PV modules. a): upper PV module in the stack, b): bottom PV module in the stack. The reduced PSDs are created according to the standard DIN EN 15433-5 Feb2008. The grey and black PSD-curves are similar standard spectra.

3.4 Vibration results from the lab

We test all types of PV modules with the ASTM D4169-09 Truck Assurance Level II PSD spectrum. We start with low mean acceleration intensity of g_{RMS}= 0.1g for 15 min. For the same PV module we increase the mean acceleration intensity for the chosen spectrum by 0.1g again for 15 min and so on up to 0.9g. In-between we measure EL, count the new cracks and classify them into the crack classes A, B and C. Fig. 11 shows the mean cumulative cracks counted for all 7 module types. The cell cracks found at 0.3g are found only for one module type. Fig. 11 also shows that the other crack types B and C occur subsequently with higher accelerations.

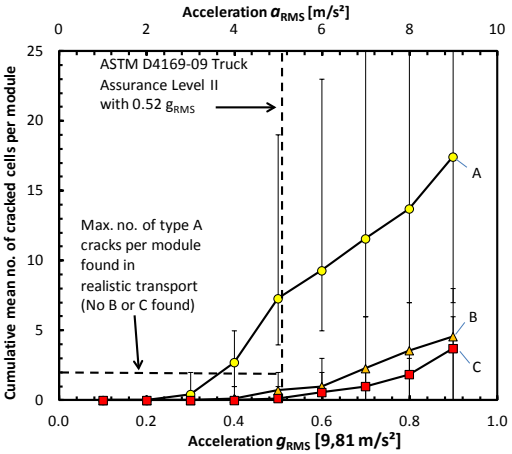

Fig. 11: The graph shows the cumulative mean number of solar cells with new cracks of type A, B and C after a 15 min noise test using the ATSM D4169-09 Truck PSD spectrum. The RMS acceleration amplitude g_{RMS} of the PSD is varied in this experiment. The bars show the maximum variance of the set of tested PV modules.

Fig. 12 shows the time dependence of the cell cracking behavior for all cell crack types. For this test we start the test with a test level of 0.4g. After almost 15 min of testing the cell cracks of type A seems to saturate for modules showing low crack sensitivity. The more crack sensitive modules seem not to fully stabilize even after 3 h of testing. They even develop to crack type B and C with rising test time. For the stabilizing module types the crack types B and C do not occur at all.

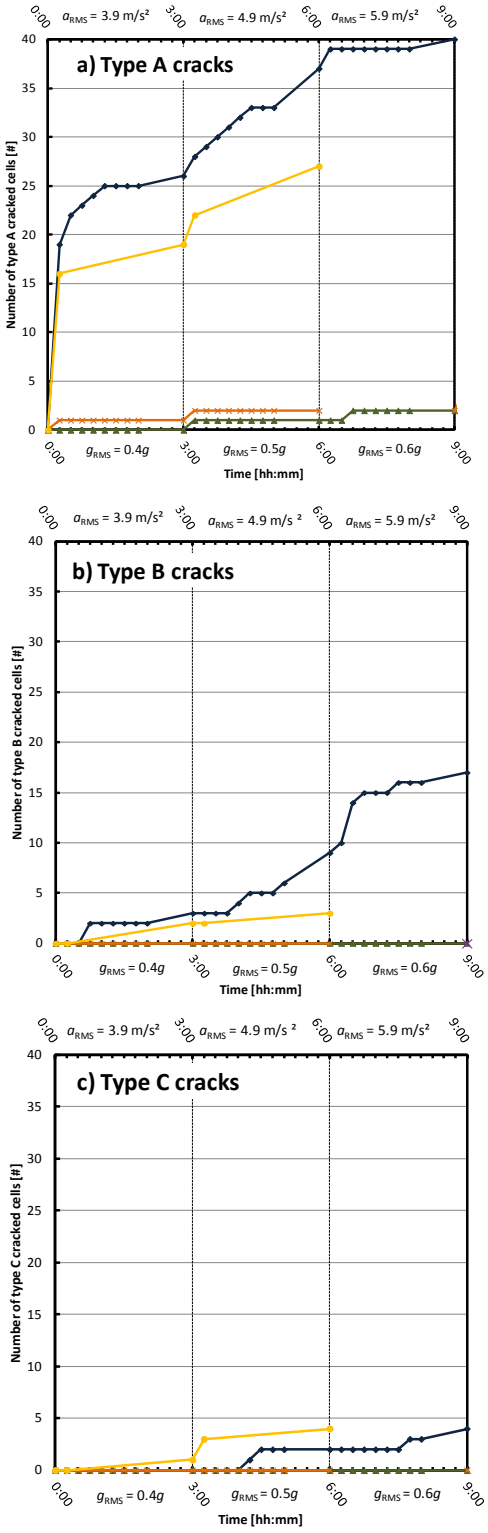

Fig. 12: The cumulative cell cracking as function of the time of the module under vibration for 4 exemplary PV module types. The mean acceleration g_{RMS} is increased after 3h and 6 h of test. Occurrence of cells showing crack type A is shown in fig a), type B in b) and type C in c).

4 DISCUSSION

The degradation caused by the transport test affects only marginally the PV module power. This result was also found by Reil et al. [2]. In this study all tests are done in a temperature range of 21°C to 27°C. During the real transportation we measured temperatures in the range of 1°C to 34°C. Due to the reason that the EVA gets much stiffer at -20°C and high frequencies [6] the impact of shocks and vibration may be much higher at even lower temperatures. Therefore cell cracking during transportation with even lower temperatures may be higher than measured in this work.
However it is still not known at which rate cell cracks develop from crack type A to crack type C. But a study on 272 of three different very old modules types shows that cell cracks are an important factor for the PV power in the wear out phase of PV modules [4].

The choice of the most suitable level of the PSD spectrum is quite critical. Even at the level of g_{RMS}=0.4g the crack number per module is in some cases higher than the maximum number of cracks found in realistic transports. However a test procedure should have a safety margin. Already a small step to g_{RMS}=0.5g increases the crack number dramatically above the level found in realistic transports. Even the PV module with the lowest number of cell cracks at g_{RMS}=0.5g shows 4 cracked cells per module after 15 min. Also some cell cracks of type B occur which are not found in realistic transports we accompanied.

One problem of the noise test may be that the test temporary brings the PV modules into resonance at low frequencies and a high level, what cannot be seen during the accompanied transports. The shock test procedure avoids the resonance problem completely.

Good modules withstand 3 h of noise test at the level of g_{RMS}=0.4g and a sine shock test with an amplitude of 30 m/s² at its maximum deflection with no or one cell crack. These both tests should be sufficient to classify a PV module to survive any transport and transport handling we accompanied. A good compromise is to combine these two tests to simulate the random transport vibration at a moderate level g_{RMS}=0.4g and test for the high amplitudes with the shock test at the modules maximum deflection with a sine shock amplitude of 30 m/s².

Due to escorting the transports or due to the mounting of the acceleration sensors we are quite sure that the truck driver handles the modules much softer than usual. Therefore our measurements are a lower assessment for the mechanical shocks during module handling. For the module transport in the truck we send the truck driver through the roughest roads we know. Therefore we think our transport route is already an upper assessment for mechanical shocks/vibrations on German roads.

5 SUMMARY AND CONCLUSION

We find that the ASTM D4169-09 Truck Assurance Level II is a well fitting PSD spectrum to simulate the vibration of PV-modules in a PV module stack during transportation. A test level of g_{RMS} = 0.4 g for the PSD spectrum is suitable for testing single modules for transportation. In our vibration test only one of seven module types showed cell cracks at g_{RMS} = 0.3g for the choosen PSD spectrum. But already at a level of g_{RMS} = 0.5 g unrealistic high cell cracking rates occur for all module types. To simulate single high shocks identified during the transportation we suggest to additionally test with sine shocks with an amplitude of 30 m/s² and a shock duration where the PV module shows its maximum

deflection. The PV modules are most sensitive to the shock duration which causes the maximum module deflection at the module middle. For 60 cell modules with glass cover and a back sheet foil the worst case sine shock duration is at about 40 ms. We showed how to build a shock transfer function for the PV module to assess the cell cracking impact of shocks. With this transfer function one can assess the impact of arbitrary shocks being measured at the module corner during real transports.

6 ACKNOWLEDGMENT

The former company SCHOTT Solar AG also took part in this project. We thank SCHOTT Solar Ag for supporting this project. We thank Dr. Arnaud Morlier for fruitful discussions about the paper.

Funding was provided by the German Federal Ministry for the Environment, Nature Conservation, and Nuclear Safety (BMU) under contract no. 0325295A (HERMES).

7 REFERENCES

[1] M. Köntges, S. Kajari-Schröder, I. Kunze and U. Jahn, “Crack Statistic of Crystalline Silicon Photovoltaic Modules,” in *Proc. 26th EUPVSEC*, Hamburg, Germany, 2011, pp. 3290 - 3294.

[2] F. Reil, J. Althaus, W. Vaaßen, W. Herrmann and K. Strohkendl, "The Effect of Transportation Impacts and Dynamic Load Tests on the Mechanical and Electrical Behaviour of Crystalline PV Modules," in *Proc. 25h European PV Solar Energy Conference*, Valencia, Spain, 06-10 September 2010, pp. 3989-3992.

[3] M. Köntges, I. Kunze, S. Kajari-Schröder, X. Breitenmoser and B. Bjørneklett, "The risk of power loss in crystalline silicon based photovoltaic modules due to micro cracks," *Sol. Energy Mater. Sol. Cells*, vol. 95, no. (4), pp. 1131-1137, 2011.

[4] K. Schulze, G. M., M. Nieß, C. Vodermayer, W. G. and G. Becker, “Untersuchung von Alterungseffekten bei monokristallinen PV-Modulen mit mehr als 15 Betriebsjahren durch Elektrolumineszenz- und Leistungsmessung,” in *Proc. 28. Symosium Photovoltaische Solarenergie*, Staffelstein, Germany, 2012.

[5] S. Kajari-Schröder, I. Kunze, U. Eitner und M. Köntges, „Spatial and orientational distribution of cracks in crystalline photovoltaic modules generated by mechanical load tests,“ *Sol. Energy Mater. Sol. Cells*, Bd. 95, Nr. (4), pp. 3054-3059, 2011.

[6] International Electrotechnical Commission (IEC) 62759: CDV, 26-07-2013. Transportation testing of photovoltaic (PV) modules – Part 1: Transportation and Shipping of Module Package Units.

[7] W. Stark and M. Jaunich, "Investigation of Ethylene/Vinyl Acetate Copolymer (EVA) by thermal," *Polymer Testing*, vol. 30, p. 236–242, 2011.